Printed ISSN 1330–0008
Online ISSN 1333–9125
CD ISSN 1333–8390
CODEN FIZAE4

MONTE CARLO SIMULATION OF RADIO FREQUENCY PLASMAS IN O_2

L. SETTAOUTI and A. SETTAOUTI

Electrotechnic Department, University of Sciences and Technology, P. O. Box. 1505, El-M'naouar, Oran, Algeria

Received 21 February 2007; Revised manuscript received 19 May 2008
Accepted 19 September 2008 Online 25 September 2008

The use of radio frequency (RF) driven discharges in many fields, including material processing, microelectronics and aerospace industry, necessitates development of effective numerical predictive tools to understand and design their behaviour. The structure of RF discharges in O_2 is examined for the electrons, positive and negative ions, where electron-neutral collisions and ion-neutral collisions are taken into consideration. Some detailed properties of radio frequency plasmas are presented using Monte Carlo simulation. The simulation results show that most of the RF external electric field is absorbed in the sheath regions. Whereas electrons respond easily to the oscillating RF electric field, ions cannot oscillate with the RF electric field. The oscillations of the electron cloud determine the instantaneous sheath thickness near each electrode. The mean energy and the density of charged particles are also discussed, and the effects of gas pressure on discharge parameters are studied.

PACS numbers: 52.20.-j, 52.25.-b, 52.65.-y UDC 533.95, 535.352

Keywords: Monte Carlo simulation, plasma, radio frequency, sheath, collision cross sections

1. Introduction

In the last few years, there has been a resurgence of interest in low pressure, radio frequency (RF) discharges as a result of their use for plasma processing in the semiconductor industry. RF plasmas are used widely for plasma etching, sputtering, film deposition and several other surface treatments in micro-electronics and recently, plasmas have also been applied as a promising candidate for large-area flat display devices. Plasma discharges have many applications as light sources with ultraviolet emissions, fluorescent lamps, dielectric barrier discharges, excimer lasers, pollution control, sterilization, biomaterial decontamination, ozone production, and in the advanced integrated circuit fabrication [1 − 7]. The unique features

of non-thermal plasmas make possible substantial breakthroughs in many high-growth areas of modern technology. It is their ability to treat surfaces effectively with minimum penetration, in a non-contact, non-destructive and highly energetic way that could lead to applications ranging from treatment of skin cancer and removal of decayed dental surfaces to material processing of low-cost polymers and semiconductors, as well as reduction of greenhouse gases [5 – 11]. New applications are continuously emerging, more noticeably in the vastly growing area of nanotechnology, which indicates that non-thermal plasma is becoming an important player in this upcoming technology. An example of such an application is the functionalization of single-walled carbon nanotubes with molecular or radical groups. This method has proven to be the most attractive because it is a clean, low-temperature process that requires minimal amount of source gas, given the efficiency of plasma sources [12 – 14]. Oxygen RF discharges are of considerable technological relevance. Industrial oxygen is currently used in plasma-assisted oxidation and ashing processes with or without adding a small number of fluorocarbon (CF) molecules. Plasmas in saturated CF molecules are generally used for etching of Si and SiO_2, and oxygen is frequently added to these plasmas to enhance the Si etch rate and to improve the selectivity. Furthermore, the ozonizer, industrial ozone generation, is a promising water purification technology. In addition, O_2 is a major component in plasma processes that are being developed for the etching of organic, low-dielectric-constant thin films. These materials are being explored as candidates for future use as interlayer dielectrics in high-speed circuits. Oxygen discharges at low-pressure are of great interest for thin-film deposition, surface activation and cleaning in electronics. Most molecular gases, such as oxygen, chlorine, SF_6, and fluorocarbons, which are used extensively for various applications of plasma processing, produce negative ions in discharges. The presence of negative ions complicates the discharge phenomena. In this study, an oxygen plasma is employed as an example of an electronegative discharge since oxygen plasmas have found numerous applications in plasma processing, such as plasma enhanced chemical vapour deposition, reactive sputtering, dry etching of polymers, oxidation, sterilization, and resist removal of semiconductors [15 – 21].

In spite of their extensive usage and technological importance in the microelectronic industry, plasma processing equipment has been empirically designed and statistically optimized at great expense of development time and cost. Due to the complexity of the plasma processes, mathematical modelling and numerical simulations are essential tools that can be used to increase our fundamental understanding and to optimize the processes. The optimization of existing processes, or the development of new processes that offer better results, may follow such an understanding. Additionally, such modelling and simulations can also be used in the computer-aided design of new process systems and to optimize existing manufacturing processes. Plasma modelling is complicated in general; it involves the solution of neutral and charged particle kinetics, radiation transport, Maxwell equations and large numbers of volume and surface reactions. Different time and spatial scales have to be resolved simultaneously and self-consistently. Incorporating all aspects of plasma in one detailed model would, therefore, result

in an untreatable model. Despite these difficulties, plasma modelling has become a valuable tool for understanding plasma physics and has contributed to the development of improved-performance plasma reactors/devices [22 – 28]. Fluctuations in RF plasmas make experimental investigation of their properties in space and time difficult. The Monte Carlo method has become a standard simulation technique for gas discharges in etching or deposition plasma reactors. Unlike the fluid approach, the Monte Carlo algorithm requires large computer resources, but it provides a detailed kinetic picture of the processes in a gas discharge [27, 28]. Monte Carlo simulation has become increasingly important as a simulation tool particularly in the area of low-temperature plasma physics.

In this paper we present a computational technique for the simulation of electrical discharge phenomena. The technique is applied to the simulation of the avalanches, the formation of the plasma and the sheaths in RF discharges in O_2. The simulation described is a Monte Carlo method in which the ions and electrons are both treated as particles; the technique also accounts for rapid spatial and temporal space-charge variations and describes the effects of gas pressure on discharge parameters.

2. *Simulation method*

Monte Carlo methods as applied to gas discharge problems involve evaluating the percentage of a given species of particles emanating from a given source, after experiencing energy loss and gain and terminating in defined categories. Its technique is realistic because a large number of particles are followed from the source throughout their life history. In any volume of gas, there exist free electrons that are caused by cosmic rays, natural radioactivity and the detachment of negative ions. An initial group of ions and electrons, typically 100 – 500, are initially randomly seeded between the electrode plates. The initial distributions of charged particles are assumed to be Maxwellian distribution of 5 eV for electrons and 0.05 eV for ions. The electrode system is assumed to consist of parallel plates with a diameter that is larger than the electrode separation. Electron and ion trajectories are computed using the Monte Carlo method [27 – 29] in a molecular gas (O_2), considering over many RF cycles the applied oscillating RF electric field which provides a time and spatially-dependent electric field. The three-dimensional motion of electrons and ions between two successive collisions under the electric field is solved numerically using the Euler method. The distribution of the electric field is calculated from the solution of the Poisson's equation with the use of the electron and ion densities at the end of each time step.

The electric field $E(z,t)$ in the direction of the z-axis (perpendicular to the electrodes) is supposed to be constant in each cell ($\Delta z = d/N_c$), where Δz is the thickness of the cell, d is the distance between electrodes and N_c is the total number of the cells. Electron flight time between two successive collisions is determined by the electron collision cross section with O_2 neutral particles. The probability of

collision in the time step Δt is

$$P = 1 - \exp\left[-\frac{\Delta t}{T_m}\right] . \tag{1}$$

The mean collision-free flight time of an electron, T_m, moving with a drift velocity $v(\varepsilon)$, is given by

$$T_m = \frac{1}{NQ_t(\varepsilon)v(\varepsilon)} , \tag{2}$$

where Q_t is the total collision cross section, N is the gas number density and ε is the electron energy. Since the heavier ions are almost stationary in the time scale of motion of electrons, a longer time scale was employed for the motion of ions. Time steps for the three-dimensional motion are chosen to be Δt for electrons and $4\Delta t$ for ions. During the successive time steps, for every electron and ion, certain information (velocity, position, etc.) is stored in order to calculate, by appropriate sampling methods, electron and ion densities, the electric field and the mean energy of electrons and ions.

The collision is simulated by comparing the probability of collision P at the end of each step with R_1, where R_1 is a random number uniformly distributed between 0 and 1. If $P < R_1$, no collision occurs and the electron or ion is followed during the next time step, if $P \geq R_1$, a collision takes place. To determine the nature of the collision, the total collision cross section Q_t is split up into its component collision cross sections for all possible collision processes of the electron, and the fractional probability of a certain kind of collision is computed. The type of collision is determined by generating a random number R_2, also uniformly distributed between 0 and 1. The segment into which R_2 falls determines the type of collision that has occurred. When no new particles are produced, the electron looses the energy corresponding to the type of collision. However, in the case of an ionizing collision, after subtracting the threshold energy, the remaining energy is evenly ascribed to the two electrons.

At a given energy ε, the sum of the fractional probabilities is equal to unity, and the interval $[0, 1]$ is divided into segments of lengths corresponding to these fractional probabilities. The nature of the collision is determined in the following way: P_j is the probability that the collision process j (the elastic, attachment, rotational, vibration, excitation and the ionization collisions) takes place, $j = 1,\ 2,\ 3, \ldots, n$,

$$P_j = \frac{Q_j}{Q_T}, \qquad \sum_j P_j = 1, \qquad P_1 + P_2 + \cdots + P_{j-1} < R_2 \leq P_1 + P_2 + \cdots + P_j . \tag{3}$$

In this way is determined the type of the jth collision process. After the collision, the particle follows its way in the next time step and the procedure is repeated. The energy of an electron after the elastic collision with a neutral molecule is given by

$$\varepsilon_1' = \varepsilon_1 \left[1 - 2\frac{m_e}{M}(1 - \cos\theta)\right] , \tag{4}$$

where ε_1 is the electron energy before the collision, m_e and M are the masses of electron and O_2 neutral molecule, respectively, and θ is the scattering angle of the electron. The energy of an ion after the elastic collision with a neutral molecule is given by [30]

$$\varepsilon'_{i1} = \varepsilon_{i1} \left[1 - \cos^2 \varphi)\right] , \tag{5}$$

where ε_{i1} is the ion energy before collision and φ the scattering angle of the ion. The scattering in all collisions is assumed to be isotropic. Charge production at the electrode surface is always important; the electron emission properties of the cathode are of primary importance. The electron yields of cathode materials, especially under gas discharge conditions, are perhaps the least known data of gas discharge physics. The secondary electron emission coefficient due to positive ions flowing to the two electrodes is assumed [31] to be 0.1. In this simulation, a sufficient number of cycles of RF are calculated for establishment of the plasma and the sheaths.

The total number of particles (electrons or ions) in the gap increases by many orders of magnitude, and it requires excessive CPU time to follow it. To circumvent this limitation, a renormalization and weighing procedure has been developed which maps the particle assembly into another consisting of fewer test particles. When the total number of simulation particles exceeds the maximum allowable number of simulation particles (which depends on the computational resources utilized for the simulation), the latter being specified with the program input data (10^5 particles), a statistical subroutine is introduced to choose an approximately equivalent group containing fewer simulation particles which replace the existing group of simulation particles. Each new particle represents several times as many actual electrons or ions of the old particles. The subroutine contains a weighting of electron velocity distribution of the old group of electrons and the ion velocity distribution of the old group of ions, so that the new group is equivalent in phase and space to the old group.

3. *Results and discussion*

We present typical results of numerical simulations using a Monte Carlo method of RF plasmas sustained by an RF external source of 13.56 MHz and an amplitude of 200 V applied to the electrodes. Oxygen is used as a working gas. The electrode system is assumed to consist of parallel plates with a diameter that is larger than the electrode separation. The calculations are performed at an electrode separation of 4 cm and the gas pressure operation range is $0.1-0.3$ Torr[1]. A summary of all electron collision cross sections [32 − 35] of O_2 employed is shown in Fig. 1. The cross sections of ion - O_2 neutral molecule collisions used here are the set for charge transfer and detachment. The cross sections of these processes as a function of the ion energy are adapted from Ref. [32] and are presented in Fig. 2.

The electric field in the first cycle oscillates with a period corresponding to the RF cycle (Fig. 3). The maximum of the electric field in the first RF cycle creates a maximum in the average electron energy, and the minimum of the average

[1]Torr is not an SI unit; it corresponds to 133 Pa (pascals).

electron energy is located in the minimum of the electric field. In the first cycles, the influence of the space charge on the applied RF electric field is not yet important. The electron density is low at the beginning of the avalanche growth, but as

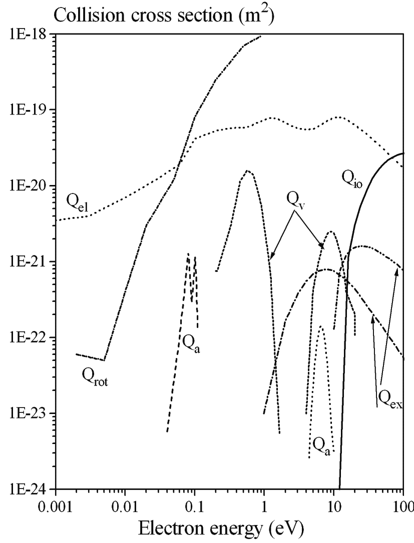

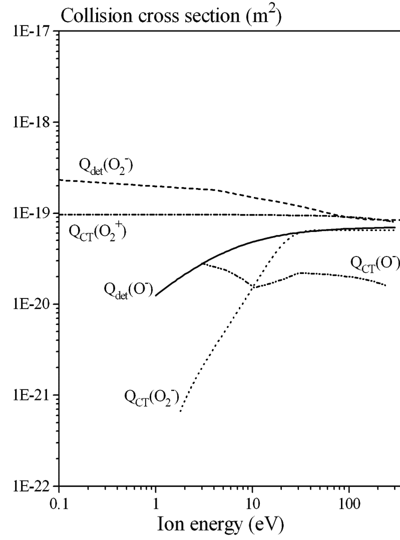

Fig. 1 (left). Collisional electron – O_2 cross sections: Q_a - attachment, Q_v - vibration, $Q_{\rm rot}$ - rotation, $Q_{\rm ex}$ - electronic excitation, $Q_{\rm io}$ - ionization, $Q_{\rm el}$ - elastic.

Fig. 2. Collisional ion – O_2 cross sections: $Q_{\rm CT}$ - charge transfer; $Q_{\rm det}$ - detachment.

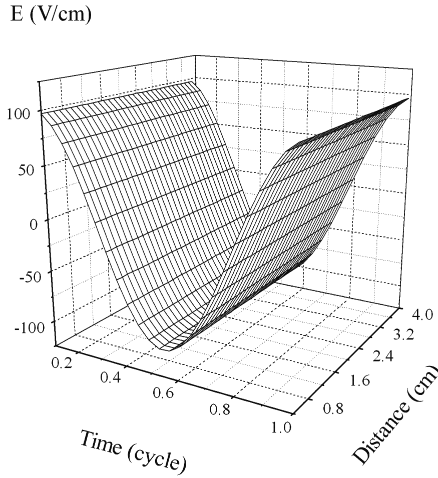

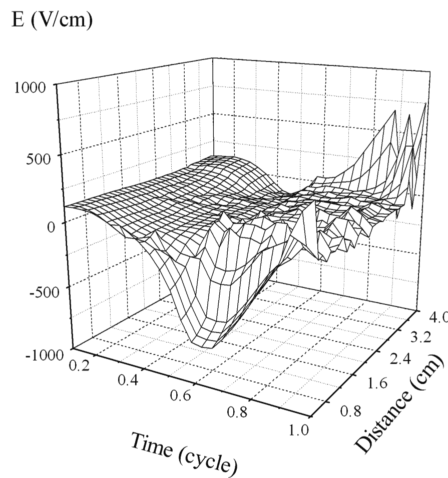

Fig. 3 (left). Temporal and spatial variations of the electric field for the first RF cycle at the pressure 0.3 Torr.

Fig. 4. Temporal and spatial variations of the electric field when the space charge field distortion begins at the pressure 0.3 Torr.

time increases, the enhancement becomes greater, and the electrons oscillate with the change in the direction of the electric field. When the applied electric field is sufficiently strong, the electron accelerates to high enough kinetic energies that inelastic collisions between the electron and the background gas occur. As the electron proceeds from the cathode to the anode, driven by the applied electric field, it undergoes many ionizing collisions in each of which an ion and a free electron are formed. Thus, we obtain an expanding cloud of electrons travelling toward the anode, known as electron avalanche, and a cloud of ions, remaining behind, and the space charge field distortion begins (Fig. 4).

An exponential increase in the electron and ion densities is caused by increasing ionization. Note that the RF electric field causes a periodic change of the density. The electron and the ion densities do not increase at $\pi/2$, $3\pi/2$ of the RF cycle when the electric field is 0. The charged particle densities increase at other points during the RF cycle and later as the field is intensified by sheath formation. At the beginning of the growth of the avalanche, the electron density is low, and as time increases, the enhancement becomes greater and the electron density oscillates with the change in the direction of the electric field. A sheath is not formed immediately and the electric field exists throughout the gap as the simulation is started with a very low charged-particle density. An exponential increase in electron and ion densities is observed followed by the sheath formation and evolution to the steady state. When the plasma is established, electrons are contained in the plasma in part by the space-charge fields. The electric field in the bulk region (in the middle of the discharge gap) is almost spatially constant and oscillates with finite amplitude and a period corresponding to the RF cycles (Fig. 5). We also note that the electric

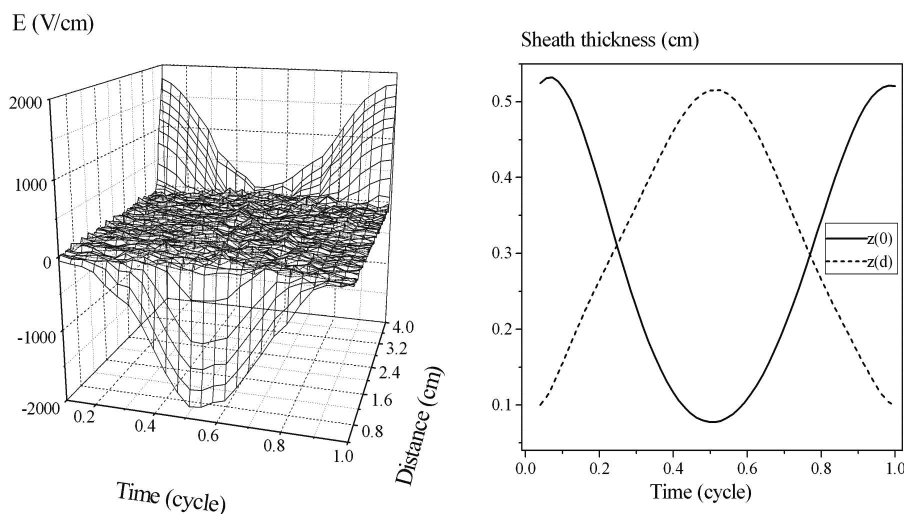

Fig. 5 (left). Temporal and spatial variation of the electric field in the RF cycle (when the plasma is established) at the pressure 0.3 Torr.

Fig. 6. Sheath thickness at both electrodes, $z(0)$ and $z(d)$ as functions of time at the pressure 0.3 Torr.

field in the sheath regions, adjacent to the electrodes, oscillates with a significant amplitude with a period corresponding to that of the RF cycles (Fig. 6). Most of the RF external electric field is absorbed in the sheath regions (Figs. 5 and 7). The electric field in the sheath changes almost linearly from both electrodes to the edge region of the bulk plasma. The electric field in the sheath has always such a direction that it repels electrons from and attracts positive ions towards the electrodes (the direction of the field is always pointed towards the electrode). There are two distinct regions in a parallel plate RF discharge, the bulk plasma and the sheaths.

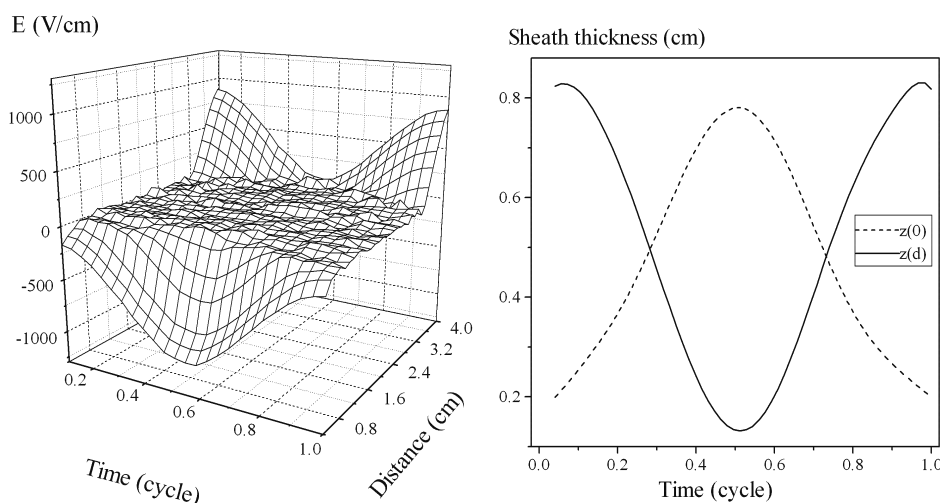

Fig. 7 (left). Temporal and spatial variation of the electric field in the RF cycle (when the plasma is established) at the pressure 0.1 Torr.

Fig. 8. Sheath thickness at both electrodes, $z(0)$ and $z(d)$ as functions of time at the pressure 0.1 Torr.

It is now widely recognised that the basic of boundary-plasma interaction physics plays a major role in the development of plasma-based technology of industrial applications. The sheath has been the main focus of low-temperature plasma applications because it is commonly used for etching of semiconductor materials and sputter deposition of thin films. In recent years, there has been considerable interest in understanding the dynamics of the discharges because the requirements for finer etching patterns or for more controlled deposition processes dictate a more systematic approach to the design of these systems. As we know, the sheath plays a crucial role in controlling the movement of the charged particles towards the electrodes. Thus, it is important to study the spatio-temporal variations of the sheath width, the ion flux and the electric field across the RF sheath. The sheath width is defined as the distance from the electrode to the edge region of the bulk plasma. The movement of electrons causes a modulation of the sheath width as shown in Figs. 6 and 8. In fact, the oscillations of the electron cloud determine the instanta-

neous sheath thickness near each electrode. When, for example, the RF electrode becomes increasingly negative, the electrons move away from the neighborhood of the RF electrode and the RF sheath is said to be in expansion. The thickness of the positive space-charge region near the RF plate is then growing. Simultaneously, the electron cloud gets closer to the opposite plate yielding a reduction in thickness of that positive space-charge region, i.e. a contraction of the opposite sheath. Note that the phase shift between the temporal behaviour of the two sheaths is π radian which is shown in Fig. 6.

An electron approaching a sheath from out of the plasma is reflected, returning to the plasma with nearly its incident energy. However, for electrons resulting from ionizations within the sheath or from secondary processes at the electrodes, these electrons are accelerated out of the sheath, gaining in energy a value nearly equal to the sheath potential. The negative ions are confined to the bulk plasma by the RF sheaths. Simulations were performed to outline the effect of gas pressure on discharge parameters. Figures 5 and 7 show the temporal and spatial contour plot of the electric fields produced at the pressures 0.3 Torr and 0.1 Torr. An observation of these figures show that the volume occupied by the plasma increases with the gas pressure (and the sheath thickness reduces). An approximate relation for the sheath thickness in the sheath regions, adjacent to the electrodes can be estimated as

$$l_S = a \pm b \cos(2\pi f t)\,, \qquad (6)$$

where l_S is the sheath thickness, a and b the constants, f the RF frequency, the sign (+) for the sheath region adjacent to the electrode $z = d$, and the sign (−) for the sheath region adjacent to the electrode $z = 0$. The opposite signs indicate that the phase shift in the temporal behaviour of the two sheaths is π. The sheath thickness results obtained by the Monte Carlo technique show that the sheath width is proportional to $p^{-1/3}$. As the pressure increases, the sheath width decreases (Figs. 6 and 8). Electron densities as functions of location and pressure are presented in Figs. 9 and 10.

Depending on the phase of the applied potential, electrons move toward one or the other electrode, their movement affects the local field causing electrons to pile up in the bulk − sheath interface. Thus, peaks appear in the electron density, the electron density has small peaks around the two sheath edges (Fig. 9), while it is almost constant in time and becomes spatially flat in the bulk region, and electrons are contained in the plasma. Electron densities as functions of location for the two O_2 discharges are presented in Fig. 10. As the O_2 pressure is increased from 0.1 Torr to 0.3 Torr, the electron densities increase. The ions are involved and widely used in industrial application of plasma-assisted techniques, such as surface coating with reactive sputtering, chemical vapour deposition process and plasma etching process. The study of ion plasma is essential to acquire proper knowledge about these physical processes. In plasma processing, a good understanding of the characteristic properties of the plasma sheath formed near a physical boundary is required to have a proper control over the parameters governing the surface

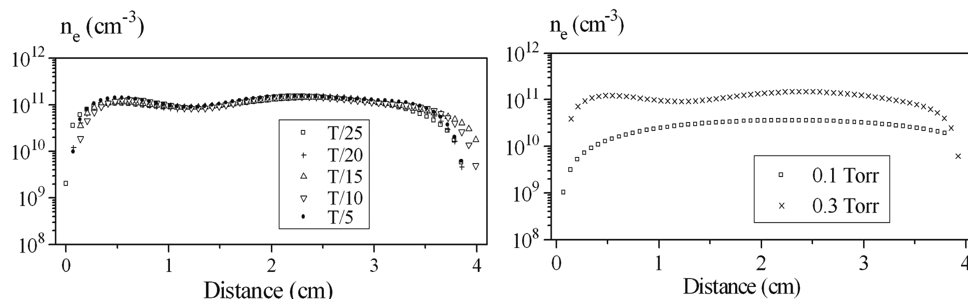

Fig. 9 (left). Electron density as a function of position at different times (T is the RF cycle) at the pressure of 0.3 Torr.

Fig. 10. Electron density as a function of position for two pressures.

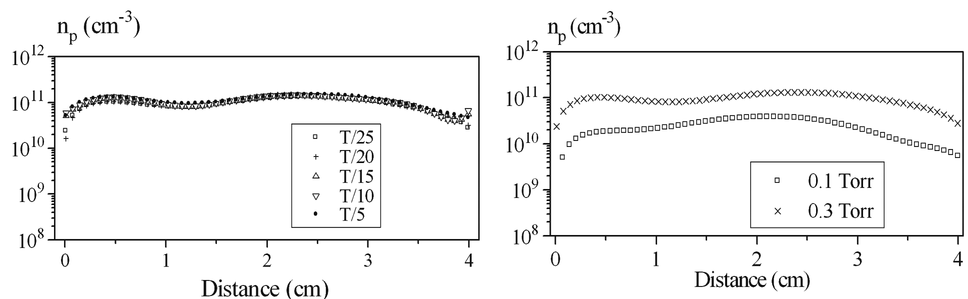

Fig. 11 (left). Positive ion density as a function of position for different times (T is the RF cycle) at the pressure 0.3 Torr.

Fig. 12. Positive ion density as a function of position for two pressures.

processes. The positive ion density (Fig. 11) is almost constant in time in both the sheath and the bulk regions, and is almost spatially uniform in bulk with small peaks around the two sheath edges. As the O_2 pressure is increased (Fig. 12), the positive-ion density increases.

In the sheath region, the positive-ion density is always higher than the negative-charge density, and hence the sheath in the present study is an ion sheath having net positive charge (Figs. 9, 11 and 13). Positive and negative charges have approximately the same densities in the bulk of the plasma, and they differ only in the thin sheath near the electrodes. The negative ions are confined to the bulk plasma by the RF sheaths and are lost primarily in ion-ion neutralization collisions and detachment collisions in the plasma volume. Thus the quasi-neutrality is respected in the discharge bulk. As the O_2 pressure is increased from 0.1 Torr to 0.3 Torr, the negative-ion densities increase (Fig. 14).

The profiles of the mean energy of the charged particles show the different nature of the three regions in the discharge. The electron mean energy is low through the plasma bulk region, and the relatively large modulations take place in the sheath

regions. The maximum in the electric field in the sheath regions creates a maximum

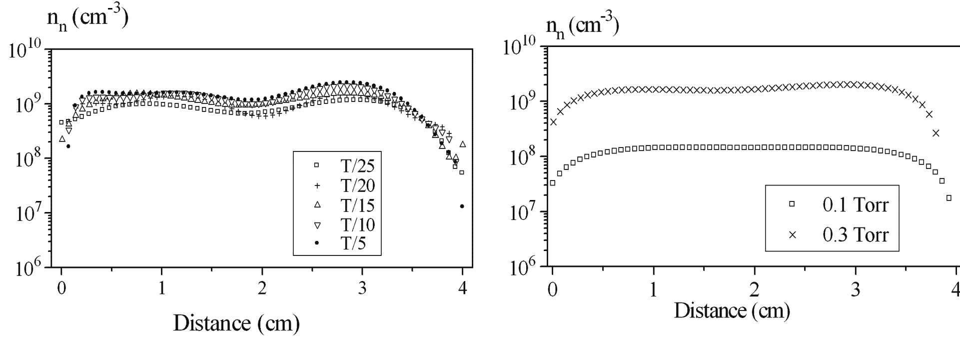

Fig. 13 (left). Negative ion density as a function of position for different times (T is the RF cycle) at the pressure 0.3 Torr.

Fig. 14. Negative ion density as a function of position for two pressures.

in the average electron energy (Fig. 15). The electron temperature increases with decreasing pressure (Figs. 15 and 16). Figure 17 and Fig. 18 show that there are two distinct regions in a parallel plate RF discharge, the bulk plasma and the sheaths. The mean ion energies (Figs. 17 and 18) are almost constant in time in both the sheath and bulk regions, and are almost spatially uniform in the bulk.

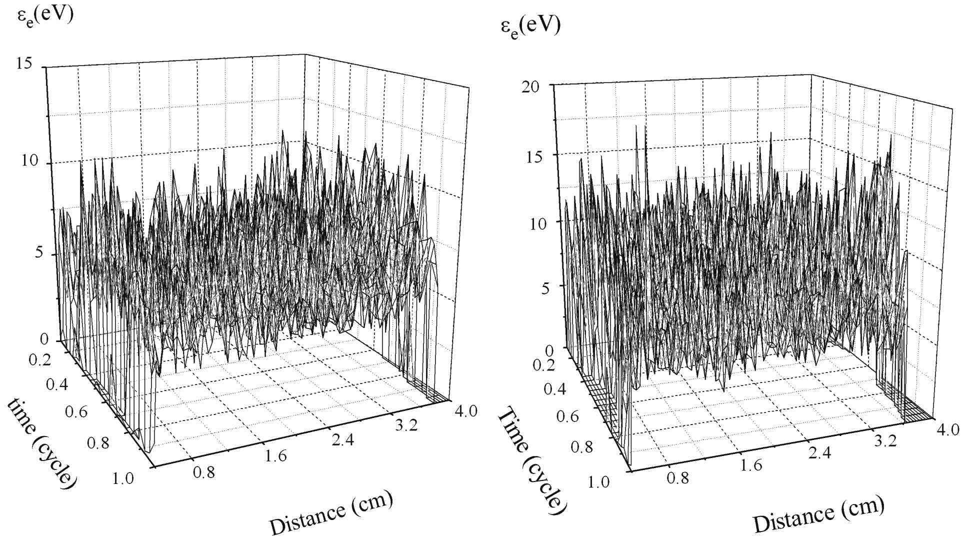

Fig. 15 (left). Temporal, and spatial variation of the mean energy of electrons at the pressure 0.3 Torr.

Fig. 16. Temporal, and spatial variation of the mean energy of electrons at the pressure 0.1 Torr.

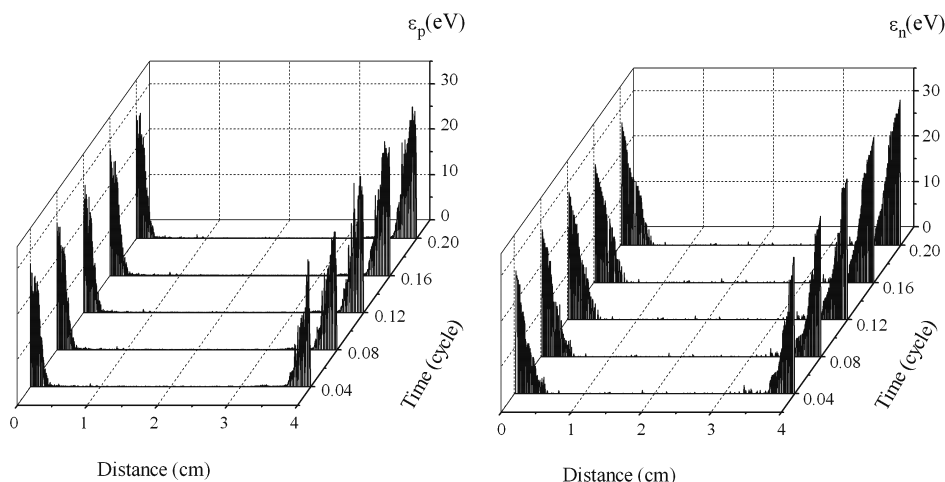

Fig. 17 (left). Temporal, and spatial variation of the mean energy of positive ions at the pressure 0.3 Torr.

Fig. 18. Temporal, and spatial variation of the mean energy of negative ions at the pressure 0.3 Torr.

Since ions cannot follow the oscillating RF electric field of 13.56 MHz, they are accelerated towards the electrodes only by the DC component of the electric field due to the potential drop in the sheath region. The energy distribution of the ions is increasingly characterized by higher energies as the ions approach the electrodes and the ions see strong electric fields in the sheath.

The discharge parameters are symmetric about the discharge mid-plane because we assumed that the geometry consists of infinite plane parallel electrodes. The calculated electric field and sheath thickness with the Monte Carlo technique compared with the result obtained in Refs. [15, 36 – 42] show a good agreement for the electric field profile, and the dependence of the sheath width on gas pressure. The agreements are found for the resulting waveform for the sheath voltage during the RF period. Almost all of the applied voltage is dropped across the sheaths at the discharge electrodes, with the results referred above. An agreement has been obtained between our results for the charged particles densities and the values reported in Refs. [19, 20, 25, 36, 37,40 – 43]. The calculated values derived from the Monte Carlo method of the mean energy of the charged particles compared with the results obtained in Refs. [19, 20, 23, 37, 40, 41], show a good agreement. The energy distribution of ions is increasingly characterized by higher energies as the ions approach the electrodes because the ions see high electric fields in the sheath.

As in most areas of computational plasma and discharge physics, it is possible to describe the physical processes in the discharge with a variety of approaches. Kinetic schemes are intrinsically higher-dimensional than fluid models since kinetic schemes involve solutions in velocity space as well as physical space and time. Kinetic models are essential for accurate description of the energy and velocity

distributions of the particle species in plasma. Computer simulations of plasmas with Monte Carlo particle codes play important role in research where a large number of parameters are involved, for example the transport phenomenon, the heating processes and the production processes through collisions and so on. In such situations, analytical solutions can not be obtained. All other things being equal, in general, kinetic schemes are computationally much more costly than fluid models, but they provide vastly more information.

4. *Conclusion*

We have developed a numerical code to illustrate Monte Carlo simulation predictions of RF plasmas for two pressures in an electronegative (O_2) model gas. We have presented typical numerical results obtained using our simulation code, and have shown the detailed properties of RF plasmas in O_2 gas, sustained by an RF external source. There are two distinct regions in a parallel plate RF discharge, the bulk plasma and the sheaths. The electric fields in the bulk are small and most of the voltage difference is concentrated in the sheaths. Note that quasi-neutrality is respected in the discharge bulk (plasma). The discharge parameters are symmetric about the discharge mid-plane because we assumed that geometry consists of infinite plane parallel electrodes. The model is in good qualitative agreement with experimental measurements.

References

[1] R. P. Mildren and R. J. Carman, J. Phys. D: Appl. Phys. **34** (2001) L1.

[2] U. Kogelschatz, IEEE Trans. Plasma Sci. **30** (2002) 1400.

[3] D. Hash, D. Bose, T. R. Govindan and M. Meyyappan, J. Appl. Phys. **93** (2003) 6284.

[4] A. Bogaerts and R. Gijbels, Vacuum **69** (2003) 37.

[5] E. M. van Veldhuizen and W. R. Rutgers, J. Phys. D: Appl. Phys. **35** (2002) 2169.

[6] E. Stoffels, A. J. Flikweert, W. W. Stoffels and GMW. Kroesen, Plasma Sources Sci. Technol. **11** (2002) 383.

[7] R. Rahul, O. Stan, A. Rahman, E. Littlefield, K. Hoshimiya, A. P. Yalin, A. Sharma, A. Pruden, C. A. Moore, Z. Yu and G. J. Collins, J. Phys. D: Appl. Phys. **38** (2005) 1750.

[8] C. P. Klages, K. Hoepfner, N. Klaeke and R. Thyen, Plasmas Polym. **5** (2000) 79.

[9] U. Kogelschatz, Plasma Sources Sci. Technol. **11** (2002) A1.

[10] K. Takaki and T. Fujiwara, IEEE Trans. Plasma Sci. **29** (2001) 518.

[11] M. Laroussi, I. Alexeff and W. L. Kang, IEEE Trans. Plasma Sci. **28** (1998) 184.

[12] B. N. Khare, M. Meyyappan, J. Kralj, P. White, M. Sisay, H. Imanaka, J. Koehne and C. W. Jr Baushchlicher, Appl. Phys. Lett. **81** (2002) 5237.

[13] M. Meyyappan, L. Delzeit, A. Cassell and D. Hash, Plasma Sources Sci. Technol. **12** (2003) 205.

[14] F. Massines, P. Segur, N. Gherardi, C. Khamphan and A. Ricard, Surf. Coat. Technol. **174** (2003) 8.

[15] N. C. M. Fuller, M. V. Malyshev, V. M. Donnelly and I. P. Herman, Plasma Sources Sci. Technol. **9** (2000) 116.

[16] T. Sakamoto, K. Naoi, H. Matsuura and H. Akatsuka, Jpn. J. Appl. Phys. **45** (2006) 243.

[17] D. Y. Kim, J. M. Kim, J. S. Jung, J. Y. Kwon, H. S. Cho, K. B. Park, H. Lim and T. Noguchi, Jpn. J. Appl. Phys. **45** (2006) L74.

[18] H. Huang, O. K. Tan, Y. C. Lee, M. S. Tse, J. Guo and T. White, Nanotechnology **17** (2006) 743.

[19] Z. Kissovski, T. Tsankov, D. Korzec, S. Kytzia and J. Engemann, Plasma Sources Sci. Technol. **15** (2006) 126.

[20] J. A. Wagner, and H. M. Katsch, Plasma Sources Sci. Technol. **15** (2006) 156.

[21] L. Xu, F. Terashita, H. Nonaka, A. Ogino, T. Nagata, Y. Koide, S. Nanko, I. Kurawaki and M. Nagatsu, J. Phys. D: Appl. Phys. **39** (2006) 148.

[22] H. C. Kim, Y. T. Sul and V. I. Manousiouthakis, IEEE Trans. Plasma Science, **32** (2004) 399.

[23] H. C. Kim, F. Iza, S. S. Yang, M. Radmilovic-Radjenovic and J. K. Lee, J. Phys. D: Appl. Phys. **38** (2005) R283.

[24] H. Takekida and K. Nanbu, J. Phys. D: Appl. Phys. **38** (2005) 3461.

[25] R. N. Franklin, J. Phys. D: Appl. Phys. **38** (2005) 2790.

[26] Z. L. Liu, X. B. Jing and K. L. Yao, J. Phys. D: Appl. Phys., **38** (2005) 1899.

[27] K. Nanbu, Jpn. J. Appl. Phys. **33** (1994) 4752.

[28] K. Nanbu, IEEE Trans. Plasma Sci. **28** (2000) 971.

[29] A. Settaouti and L. Settaouti, Fizika A (Zagreb) **13** (2004) 121.

[30] A. Bogaerts, PhD thesis, University of Antwerpen, 1996.

[31] A. Bogaerts and R. Gijbels, Plasma Sources Sci. Technol. **11** (2002) 27.

[32] J. L. Delcroix, *Physique des plasmas*, tome 2, Dunod, Paris, 1966.

[33] Y. Itikawa, A. Ichimura, K. Onda, K. Sakimoto, K. Takayanagi, Y. Hatano, M. Hayashi, H. Nishimura and S. Tsurubushi, J. Phys. Chem. Ref. data **18** (1989) 23.

[34] S. Kajita, S. Ushirata and Y. Kondo, J. Appl. Phys. **67** (1990) 4015.

[35] B. H. Jeon, J. Korean Phys. Soc. **43** (2003) 513.

[36] S. Dine, J. P. Booth, G. A. Curley, C. S. Corr, J. Jolly and J. Guillon, Plasma Sources Sci. Technol. **14** (2005) 777.

[37] A. H. Sato and M. A. Lieberman, J. Appl. Phys. **68** (1990) 6117.

[38] U. Deka, R. Prakash, A. Sarma and C. B. Dwivedi, Jpn. J. Appl. Phys. **43** (2004) 2704.

[39] K. Denpoh, G. Wakayama and K. Nanbu, Jpn. J. Appl. Phys. **43** (2004), 5533.

[40] M. J. Goeckner, J. Goree and T. E. Sheridan, Phys. Fluids B **4** (1992) 1663.

[41] M. A. Sobolewski, Appl. Phys. Lett. **70** (1997) 1049.

[42] Y. W. Choi and H. J. Lee, IEEE Trans. Plasma Science **31** (2003) 1032.

[43] A Brockhaus, G F Leu, V Selenin, Kh Tarnev and J Engemann, Plasma Sources Sci. Technol. **15** (2006) 171.

MONTE CARLO SIMULACIJA RADIOFREKVENTNE PLAZME U O_2

Primjena izboja s radiofrekventnom (RF) uzbudom u mnogim područjima, kao što su obrada materijala, mikroelektronička i svemirska industrija, zahtijeva razvoj učinkovitih numeričkih alata za razumijevanje, predviđanje i programiranje njihovih svojstava. Proučavamo strukturu RF izboja u O_2 za elektrone, te pozitivne i negativne ione, razmatrajući sudare elektrona i iona s neutralnim molekulama. Opisujemo podrobno neka svojstva RF plazme primjenom Monte Carlo simulacije. Ishodi simulacije pokazuju da je vanjsko RF električno polje apsorbirano u području graničnih ploha. Odziv elektrona na vanjsko oscilatorno RF polje je izražen, ali ioni ne mogu pratiti brze promjene RF električnog polja. Oscilacije elektronskog oblaka određuju trenutnu debljinu granične plohe pored obje elektrode. Raspravljamo također srednju energiju i gustoću nabijenih čestica kao i učinke tlaka plina na parametre izboja.